

Room Temperature Spin Accumulation Effect in Boron Doped Si Created by Epitaxial Fe₃Si/*p*-Si Schottky Contact¹

A. S. Tarasov^{a, b}, I. A. Bondarev^{a, b, *}, M. V. Rautskii^a, A. V. Lukyanenko^{a, b}, I. A. Tarasov^{a, c}, S. N. Varnakov^{a, c}, S. G. Ovchinnikov^{a, b}, and N. V. Volkov^a

^aKirensky Institute of Physics, Federal Research Center KSC SB RAS, Krasnoyarsk, 660036 Russia

^bInstitute of Engineering Physics and Radio Electronics, Siberian Federal University, Krasnoyarsk, 660041 Russia

^cSiberian State Aerospace University, Krasnoyarsk, 660014 Russia

*e-mail: fbi1993@mail.ru

Received January 27, 2018

Abstract—To study spin-dependent transport phenomena in Fe₃Si/*p*-Si structures we fabricated 3-terminal planar microdevices and metal/semiconductor diode using conventional photolithography and wet chemical etching. I–V curve of prepared diode demonstrates rectifying behavior, which indicates the presence of Schottky barrier in Fe₃Si/*p*-Si interface. Calculated Schottky barrier height is 0.57 eV, which can provide necessary conditions for spin accumulation in *p*-Si. Indeed, in 3-terminal planar device with Fe₃Si/*p*-Si Schottky contact Hanle effect was observed. By the analysis of Hanle curves spin lifetime spin diffusion length in *p*-Si were calculated, which are 145 ps and 405 nm, respectively (at $T = 300$ K). Spin lifetime strongly depends on temperature which can be related to the fact that spin-dependent transport in our device is realized via the surface states. This gives a perspective of creation of spintronic devices based on metal/semiconductor structure without need for forming tunnel or Schottky tunnel contact.

Keywords: spintronics, hybrid structures, Schottky diode, Hanle effect, spin accumulation

DOI: 10.1134/S1027451018040171

INTRODUCTION

For realization of spin transport in ferromagnetic metal/insulator/semiconductor (MIS) structures high interface quality is required, because defects and impurities cause scattering of spin-polarized carriers. However, epitaxial growth of insulating tunnel transparent layer is a non-trivial technological task. This significantly complicates fabrication of MIS structures for spintronics. Despite the fact that tunnel transparent insulator is required for solving the conductivity mismatch problem [1], number of works demonstrate possibility of spin transport creation in ferromagnetic metal/semiconductor (MS) structures, where the role of insulator is played by the Shottky barrier [2, 3].

Fe₃Si is one of the promising materials for creation of MS structure. DO3-ordered Fe₃Si is one of the ferromagnetic (FM) Heusler compounds with 45% spin polarization at Fermi level and a Curie temperature (T_c) of 840 K. Fe₃Si epitaxial growth can be controlled easily, in comparison to three-component Heusler alloys. Furthermore, Fe₃Si can be epitaxially grown on GaAs, Ge and Si substrates [2, 4–7]. At present, spin transport in Fe₃Si/GaAs hybrid structures is mostly

studied. Interest to Fe₃Si/GaAs is caused by the fact that lattice mismatch between Fe₃Si and GaAs is less than for Ge and Si. Furthermore, GaAs has spin-orbit interaction, which potentially allows to manipulate spin current in GaAs. But on the other hand, spin-orbit interaction leads to decreasing of spin lifetime and therefore to decreasing of spin diffusion length. In Si on the contrary, spin-orbit interaction is absent, and spin diffusion length can reach the value of 350 μm [8–12]. Also, using Si as a semiconductor in hybrid structures allows integrating spin devices into traditional semiconductor electronics.

For Fe₃Si/Si, spin injection at room temperature had been already demonstrated. However, in most of the works devoted to spin injection in Si, *n*-type substrates are used, while structures based on *p*-Si are poorly studied. Earlier, we discovered some ac and dc magnetoresistive effects in *p*-Si based MIS structures [13–16], that reach gigantic values, up to 10⁷% [17]. But those phenomena don't relate directly to spin-dependent carriers' transport. In current work we present results of transport study in Fe₃Si/*p*-Si MS structure. Analysis of experimental data confirms that room temperature spin accumulation effect was realized in boron doped silicon.

¹ The article is published in the original.

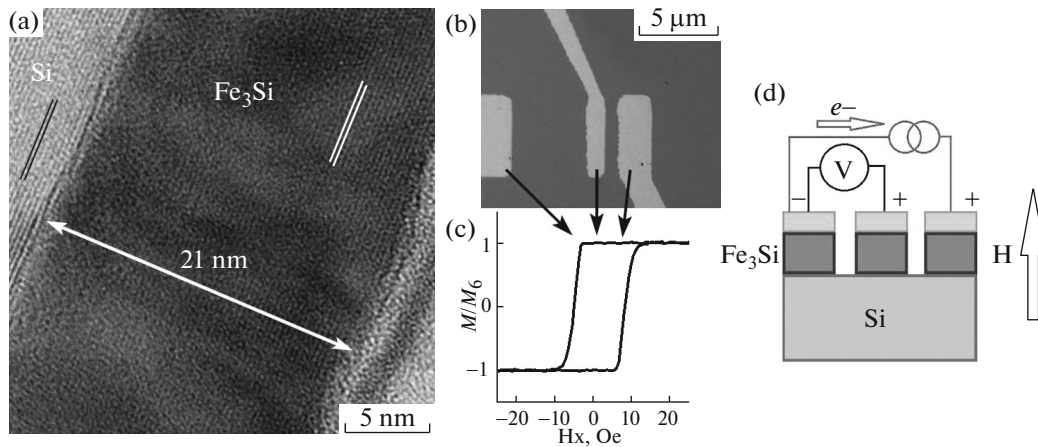


Fig. 1. (a) High resolution TEM image of the $\text{Fe}_3\text{Si}/\text{Si}(111)$ structure cross section. (b) 3-Terminal planar microstructure optic image. (c) MOKE hysteresis loops for each terminal of planar device. (d) Experimental scheme for studying Hanle effect.

EXPERIMENTAL DETAILS

The Fe_3Si film was epitaxially grown on an atomically pure boron-doped silicon substrate $p\text{-Si}(111)$ (with resistivity of $7.5 \Omega \text{ cm}$) at 400 K by molecular beam epitaxy (MBE) in ultra-high vacuum conditions (UHV) in Angara chamber [18]. The base pressure in a working chamber was $1.3 \times 10^{-8} \text{ Pa}$. Before synthesis, the substrate was chemically treated and annealed in ultra-high vacuum. First, the Si (111) wafer was gradually heated to 650°C and kept at this temperature for 15 min; then it was rapidly heated to 800°C and kept for 30s; finally, the temperature was decreased again to 650°C . This treatment was repeated until the Si (111) surface was restructured.

Fe and Si were simultaneously evaporated from two Knudsen effusion cells. The ratio between the deposition rates Si: F = 0.57 ensured the stoichiometric composition of the Fe_3Si film. Structural in situ and ex situ characterization of the films obtained was made by reflective high-energy electron diffraction, X-ray diffraction, and transmission electron microscopy (TEM), which confirmed single crystallinity and interface abruptness of $\text{Fe}_3\text{Si}/\text{Si}$ structure. More detailed information about sample fabrication and characterization can be found in [19, 20], but here we present only TEM image (Fig. 1a) which clearly demonstrates film quality.

For Hanle measurements in $\text{Fe}_3\text{Si}/\text{Si}$, we fabricated 3-terminal planar microstructures (Fig. 1b) using conventional photolithography and wet chemical etching, with solution of hydrofluoric acid and nitric acid $\text{HF} : \text{HNO}_3 : \text{H}_2\text{O} = 1 : 2 : 400$. At this concentration of etching solution and constant agitation at room temperature, the etching speed of Fe_3Si film was about 50 \AA/s . Complementary verification of etching process was probed by MOKE microscopy with the help of NanoMOKE 2 installation. For each terminal of planar microstructure individual magnetic hystere-

sis loop was measured. As seen on Fig. 1c all loops are coincide which indicate both high film quality and successful 3-terminal device fabrication with ferromagnetic electrical contacts. Transport properties and Hanle effect were studied using experimental setup, equipped with helium cryostat ($4.2 \text{ K} < T < 300 \text{ K}$), an electromagnet ($-1\text{T} < H < 1\text{T}$) and Keithley 2634b SourceMeter. Experimental scheme is presented in Fig. 1d.

RESULTS AND DISCUSSIONS

Before studying magnetic field-dependent transport properties at first we checked the main electrical characteristics of $\text{Fe}_3\text{Si}/p\text{-Si}$ structure such as film resistivity and Schottky barrier parameters. Fe_3Si film demonstrates metallic behaviour in temperature range from 4 to 300 K. In this temperature region the resistivity value rises from $55 \mu\text{Ohm cm}$ to $120 \mu\text{Ohm cm}$, which is correlate with other results reported for epitaxial Fe_3Si films [21, 22]. To identify Schottky barrier parameters I–V characteristics of prepared diode were measured. Ohmic contact on backside of silicon substrate was made by indium alloying (right inset on Fig. 2). The main panel of Fig. 2 shows the absolute value of the current density $|J|$ as a function of bias voltage. Typical rectifying behavior of a conventional Schottky diode can be seen. Direct branch of the I–V curve was analysed via Cheung's method [23], which allows to calculate the barrier height ϕ_{Bp} , ideality factor n and series resistance R_S of a Schottky barrier. Cheung's functions for voltage (U) and current density (J) containing those parametrs can be expressed as:

$$\frac{dU}{d(\ln J)} = R_S A_{\text{eff}} J + n \frac{k_B T}{q}, \quad (1)$$

$$H(J) \equiv V - n \frac{k_B T}{q} \ln \left(\frac{J}{A^{**} T^2} \right), \quad (2)$$

$$H(J) = R_S A_{\text{eff}} J + n \phi_{Bp}. \quad (3)$$

Here, A_{eff} is the effective area of the diode, A^{**} is the Richardson constant ($8.6 \text{ cm}^{-2} \text{ K}^{-2} \text{ A}$). Plot of $dU/d(\ln J)$ vs. J give us RA_{eff} as the slope and $n \frac{k_B T}{q}$ as the y -axis intercept. Using eq. (2) $H(J)$ function can be plotted to determine barrier height ϕ_{Bp} from y -axis intercept according eq. (3). Approximating both dependences showed on Fig. 3 by straight lines, ϕ_{Bp} , n and R_S values were calculated (see insets on Figs. 2 and 3). Ideality factor has relatively high value. This suggests that thermionic emission model, which lie in the basis of used I–V curve analysis method doesn't ideally describes electron transport through our M/S diode. Probably, there are some additional transport mechanisms in $\text{Fe}_3\text{Si}/p\text{-Si}$ structure, which weaken rectifying properties of the diode. As a result, low ratio of direct and reverse current is observed on I–V curve (about 25 for $U = \pm 0.3\text{V}$). Nevertheless, the most important parameter – Schottky barrier height has value of 0.57 eV which is adequate for M/S diode based on $p\text{-Si}$ substrate. It is close to similar values which were observed in both MIS [24] and MS [25] structures, including $\text{Fe}_3\text{Si}/n\text{-Si}$ epitaxial structure [25]. This can provide necessary conditions for spin injection from Fe_3Si to $p\text{-Si}$.

Spin-polarized current injection from Fe_3Si to $p\text{-Si}$ produces an imbalance in the hole population in the valence band. It can be explained by the difference of electrochemical potentials, μ^\uparrow and μ^\downarrow , for the up and down spin directions, respectively. Then the spin accumulation can be written in the form $\Delta\mu = \mu^\uparrow - \mu^\downarrow$. Maximal value of spin accumulation is observed under ferromagnetic contact. With an increase of distance from the interface, this value decreases according to spin diffusion length in silicon, L_{SD} . The orientation of the spin polarization is determined by the magnetization direction of the ferromagnetic contacts, which magnetic moment lies in sample plane. When magnetic field is applied perpendicular to the sample plane, it induces spin precession with Larmor frequency:

$$\omega_L = 2\pi g \mu_B B / h, \quad (4)$$

where g is the Lande g -factor, μ_B is the Bohr magneton and h is Planck's constant. Spin precession leads to random generation and diffusion of spin carriers, as a result spin accumulation decreases. Field dependence of spin accumulation $\Delta\mu$ has Lorentzian shape, and given by expression:

$$\Delta\mu(H) = \Delta\mu(0) / (1 + (\omega_L \tau_s)^2), \quad (5)$$

where τ_s is the spin lifetime. Application of direct current through ferromagnetic contacts 1 and 3 (Fig. 1d) will cause spin injection from Fe_3Si to Si (or extraction from Si to Fe_3Si), which will lead to spin accumulation

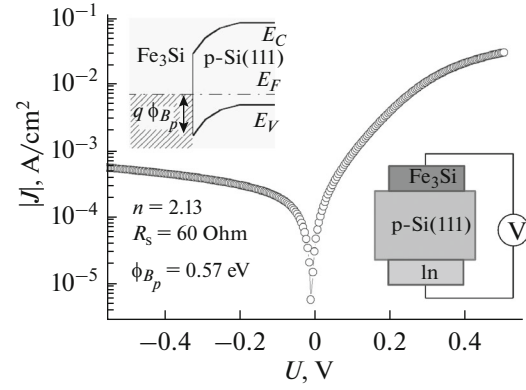


Fig. 2. I–V characteristic of the $\text{Fe}_3\text{Si}/p\text{-Si}$ Schottky diode at 295 K. The right and left insets show schematic illustrations of the experimental scheme for $\text{Fe}_3\text{Si}/\text{Si}(111)$ diode and an energy diagram of the Schottky barrier for $\text{Fe}_3\text{Si}/p\text{-Si}(111)$ structure, respectively.

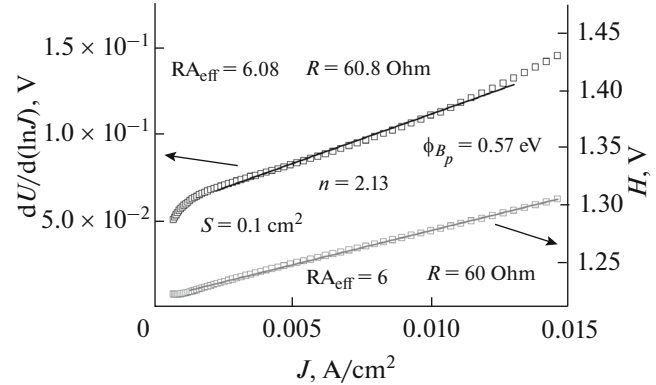


Fig. 3. Plots of $dV/d(\ln J)$ (left panel) and $H(J)$ vs. J (right panel) of the $\text{Fe}_3\text{Si}/p\text{-Si}$ Schottky diode.

in silicon. This spin accumulation can be determined by measuring 3-terminal voltage signal ΔV between 1 and 2 contacts (Fig. 1d). According to works [26–28] 3-terminal voltage signal can be defined as $\Delta V = A_{\text{sp}} \Delta\mu/2$, where A_{sp} is efficiency coefficient of spin transfer through interface ferromagnetic/semiconductor. Then, expression (5) can be written as:

$$\Delta V(H) = \Delta V(0) / (1 + (\omega_L t_s)^2). \quad (6)$$

Using experimental geometry showed on Fig. 1d measurements of direct and reverse Hanle effect [28] had been performed for 3-terminal planar device with 5 μm distance between closest FM Fe_3Si electrodes. Dependence of 3-terminal voltage vs perpendicular magnetic field is presented on Fig. 4 (solid circles). At constant dc current $I = +500 \mu\text{A}$, V monotonically decreases with an increase of magnetic field. It indicates the occurrence of spin polarization in silicon due to the spin-dependent hole extraction from silicon to Fe_3Si . External magnetic field suppresses this accumulation. Experimental data described well by

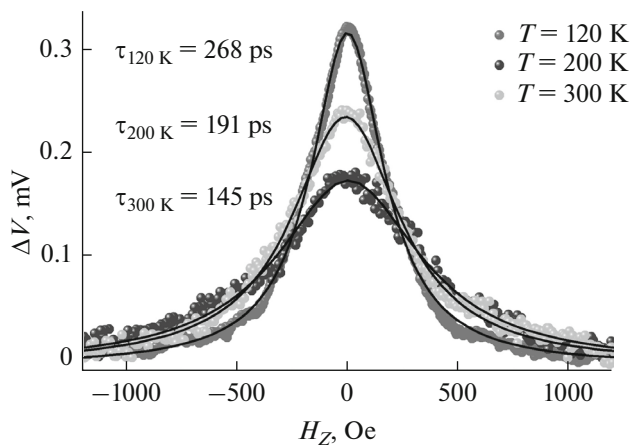


Fig. 4. Hanle curves for $\text{Fe}_3\text{Si}/p\text{-Si}$ 3-T device at $T = 300$ K; 200 K; 120 K (circles) and Lorentzians fits (solid lines).

Lorentzian line shape (6), Lorentzian fit is presented at Fig. 4 (solid lines).

By the analysis of Lorentzian curve, one can calculate spin lifetime $\tau_s = 1/\omega_L = h/2\pi g_h \mu_B \Delta B$, where ΔB is half-width of the curve in its half-max, g_h is Lande g -factor of holes ($g_h = 2$). For our devices $\tau_s = 145$ ps, 191 ps, and 268 ps, for $T = 300$ K, 200 K and 120 K, respectively. This spin lifetime values are typical for silicon. For example, for structure with an epitaxial $\text{MgO}(001)$ tunnel barrier and $\text{Fe}(001)$ electrode τ_s in highly doped p -Si is 133 ps at injection current of 0.85 mA [29]. In work [30] spin lifetime values in highly doped p -Si with Al_2O_3 tunnel barrier and different ferromagnetic electrodes are 60 ps, 110 ps, and 270 ps for Fe, Co and $\text{Ni}_{80}\text{Fe}_{20}$ electrodes, respectively. In another work [3] MS structure $\text{Fe}_3\text{Si}/n\text{-Si}$ with δ -doped layer and Schottky tunnel barrier has $\tau_s = 470$ ps.

Despite the fact that our structure doesn't have insulating tunnel barrier or Schottky tunnel contact, spin current can tunnel through surface states which are located at metal/semiconductor interface [31]. Furthermore, efficiency of spin-dependent tunneling depends weakly on temperature, and changing of carriers' mobility can't increase spin lifetime more than 30–50% [28]. In our case, with decreasing of temperature from 300 to 120 K spin lifetime increases almost twice. This also confirms that spin-dependent tunneling is realized through the surface states [32, 33].

Knowing spin lifetime we can define the spin diffusion length $L_{SD} = \sqrt{D_h \tau_s}$. Here D_h is hole diffusion coefficient in silicon, which for our device is $11.3 \text{ cm}^2/\text{s}$ at $T = 300$ K, and the spin diffusion length value is 405 nm. It should be noted that in experiment we observe high values of ΔV . According to expression $\Delta V = A_{sp} \Delta \mu / 2$ this indicates either high efficiency of spin-dependent hole extraction from p -Si to Fe_3Si , or

high value of spin accumulation $\Delta \mu$. If we suggest that at room temperature (300 K) extraction efficiency is 10%, spin accumulation value will be 3.5 meV at $I = 0.5$ mA. These results give possibility to create spin dependent transport in MS structure based devices which will be realized via surface states.

CONCLUSIONS

High quality epitaxial Fe_3Si film was grown on a the p -Si(111) substrate. From analysis of $\text{Fe}_3\text{Si}/p\text{-Si}$ diode I–V curve, Schottky barrier height was determined, which is 0.57 eV at room temperature. Spin accumulation in p -Si was studied using 3–T Hanle method. By the Hanle curves analysis room temperature spin lifetime $\tau_s = 145$ ps and spin diffusion length $L_{SD} = 405$ nm were calculated. With decreasing of temperature to 120 K spin lifetime nearly doubles and becomes 268 ps. Strong temperature dependence of spin lifetime indicates that spin-dependent transport between Fe_3Si and p -Si is realized via surface states. Analysis of Hanle curves amplitudes allows concluding that it is possible to create spintronic devices based on MS structures without need of forming tunnel or Schottky tunnel contact. This removes some technological obstacles in a way of integration of spintronic devices into the modern semiconductor electronics.

ACKNOWLEDGMENT

The reported study was funded by Russian Foundation for Basic Research, Government of Krasnoyarsk Territory, Krasnoyarsk Region Science and Technology Support Fund to the research project nos. 16-42-243046, 16-42-242036 and 16-42-243060.

REFERENCES

1. E. I. Rashba, Phys. Rev. B **62**, R16267(R) (2000). <https://doi.org/10.1103/PhysRevB.62.R16267>.
2. Y. Ando, K. Hamaya, K. Kasahara, et al., Appl. Phys. Lett. **94** (18), 182105 (2009). <https://doi.org/10.1063/1.3130211>.
3. Y. Fujita, S. Yamada, Y. Ando, et al., J. Appl. Phys. **113** (1), 013916 (2013). <https://doi.org/10.1063/1.4773072>.
4. K. Hamaya, K. Ueda, Y. Kishi, et al., Appl. Phys. Lett. **93** (13), 132117 (2008). <https://doi.org/10.1063/1.2996581>.
5. T. Sadoh, M. Kumano, R. Kizuka, et al., Appl. Phys. Lett. **89** (18), 182511 (2006). <https://doi.org/10.1063/1.2378399>.
6. J. Herfort, H. P. Schönherr, and K. H. Ploog, Appl. Phys. Lett. **83** (19), 3912–3914 (2003). <https://doi.org/10.1063/1.1625426>.
7. Y. Ando, K. Kasahara, K. Yamane, et al., Appl. Phys. Express **3** (9), 093001 (2010). <https://doi.org/10.1143/APEX.3.093001>.
8. B. Huang, D. J. Monsma, and I. Appelbaum, Phys. Rev. Lett. **99** (17), 177209 (2007). <https://doi.org/10.1103/PhysRevLett.99.177209>.
9. P. Li and H. Dery, Phys. Rev. Lett. **107** (10), 107203 (2011). <https://doi.org/10.1103/PhysRevLett.107.107203>.

10. Y. Song and H. Dery, *Phys. Rev. B* **86** (8), 085201 (2012). <https://doi.org/10.1103/PhysRevB.86.085201>.
11. J. L. Cheng, M. W. Wu, and J. Fabian, *Phys. Rev. Lett.* **104** (1), 016601 (2010). <https://doi.org/10.1103/PhysRevLett.104.016601>.
12. J. M. Tang, B. T. Collins, and M. E. Flatté, *Phys. Rev. B* **85** (4), 045202 (2012). <https://doi.org/10.1103/PhysRevB.85.045202>.
13. N. V. Volkov, A. S. Tarasov, D. A. Smolyakov, et al., *J. Magn. Magn. Mater.* **383**, 69–72 (2015). <https://doi.org/10.1016/j.jmmm.2014.11.014>.
14. N. V. Volkov, A. S. Tarasov, M. V. Rautskii, et al., *J. Surf. Invest.: X-ray, Synchrotron Neutron Tech.* **9** (5), 984–994 (2015). <https://doi.org/10.1134/S1027451015050432>.
15. A. S. Tarasov, M. V. Rautskii, A. V. Lukyanenko, et al., *J. Alloys Compd.* **688**, 1095–1100 (2016). <https://doi.org/10.1016/j.jallcom.2016.07.138>.
16. N. V. Volkov, A. S. Tarasov, M. V. Rautskii, et al., *J. Magn. Magn. Mater.* **440**, 140–143 (2017). <https://doi.org/10.1016/j.jmmm.2016.12.092>.
17. N. V. Volkov, A. S. Tarasov, D. A. Smolyakov, et al., *AIP Adv.* **7** (1), 015206 (2017). <https://doi.org/10.1063/1.4974876>.
18. S. N. Varnakov, A. A. Lapeshev, S. G. Ovchinnikov, et al., *Instrum. Exp. Tech.* **47** (6), 839–843 (2004). <https://doi.org/10.1023/B:INET.0000049709.08368.3e>.
19. I. A. Yakovlev, S. N. Varnakov, B. A. Belyaev, et al., *JETP Lett.* **99** (9), 527–530 (2014). <https://doi.org/10.1134/S0021364014090124>.
20. A. S. Tarasov, A. V. Lukyanenko, I. A. Tarasov, et al., *Thin Solid Films* **642**, 20–24 (2017). <https://doi.org/10.1016/j.tsf.2017.09.025>.
21. H. Vinzelberg, J. Schumann, D. Elefant, et al., *J. Appl. Phys.* **104** (9), 093707 (2008). <https://doi.org/10.1063/1.3008010>.
22. H. Y. Hung, S. Y. Huang, P. Chang, et al., *J. Cryst. Growth* **323** (1), 372–375 (2011). <https://doi.org/10.1016/j.jcrysgro.2010.11.075>.
23. S. K. Cheung and N. W. Cheung, *Appl. Phys. Lett.* **49** (2), 85–87 (1986). <https://doi.org/10.1063/1.97359>.
24. M. Okutan and F. Yakuphanoglu, *Microelectron. Eng.* **85** (3), 646–653 (2008). <https://doi.org/10.1016/j.mee.2007.11.011>.
25. K. Hamaya, Y. Ando, T. Sadoh, et al., *Jpn. J. Appl. Phys.* **50** (1R), 010101 (2011). <https://doi.org/10.1143/JJAP.50.010101>.
26. A. Fert and H. Jaffrès, *Phys. Rev. B* **64** (18), 184420 (2001). <https://doi.org/10.1103/PhysRevB.64.184420>.
27. V. V. Osipov and A. M. Bratkovsky, *Phys. Rev. B* **72** (11), 115322 (2005). <https://doi.org/10.1103/PhysRevB.72.115322>.
28. S. P. Dash, S. Sharma, R. S. Patel, et al., *Nature* **462** (7272), 491–494 (2009). <https://doi.org/10.1038/nature08570>.
29. A. Spiesser, S. Sharma, H. Saito, et al., arXiv:1211.1510 [cond-mat.mtrl-sci] (2012). <https://doi.org/10.1117/12.930839>.
30. S. P. Dash, S. Sharma, J. C. Le Breton, et al., *Phys. Rev. B* **84** (5), 054410 (2011). <https://doi.org/10.1103/PhysRevB.84.054410>.
31. A. Dankert, R. S. Dulal, and S. P. Dash, *Sci. Rep.* **3**, 3196 (2013). doi 10.1038/srep03196
32. M. Tran, H. Jaffrès, C. Deranlot, et al., *Phys. Rev. Lett.* **102** (3), 036601 (2009). <https://doi.org/10.1103/PhysRevLett.102.036601>.
33. R. Jansen, A. M. Deac, H. Saito, and S. Yuasa, *Phys. Rev. B* **85** (13), 134420 (2012). <https://doi.org/10.1103/PhysRevB.85.134420>.